

Editorial Manager(tm) for Neurochemical Research
Manuscript Draft

Manuscript Number: NERE2167R1

Title: Carnosic acid, a rosemary phenolic compound, induces apoptosis through reactive oxygen species-mediated p38 activation in human neuroblastoma IMR-32 cells

Article Type: Original

Keywords: Carnosic acid; apoptosis; reactive oxygen species; p38 kinase; human neuroblastoma IMR-32 cells

Corresponding Author: Chia-Wen Tsai

Corresponding Author's Institution: China Medical University

First Author: Chia-Wen Tsai

Order of Authors: Chia-Wen Tsai; Chia-Yuan Lin, Ph.D.; Hui-Hsuan Lin; Jing-Hsien Chen

1 Carnosic acid, a rosemary phenolic compound, induces apoptosis through reactive oxygen
2 species-mediated p38 activation in human neuroblastoma IMR-32 cells

3
4
5
6
7 4 Chia-Wen Tsai . Chia-Yuan Lin . Hui-Hsuan Lin . Jing-Hsien Chen

8
9
10
11 5
12
13 6 C. W. Tsai (✉) . C. Y. Lin

14
15
16
17 7 Department of Nutrition, China Medical University, 91, Hsueh-Shih Rd, Taichung 404,
18
19 8 Taiwan
20
21
22 9 e-mail address: cwtsai@mail.cmu.edu.tw

23
24 10
25
26
27 11 H. H. Lin
28
29 12 School of Medical Laboratory and Biotechnology, Chung Shan Medical University, Taichung,
30
31 13 Taiwan

32
33
34 14 Department of Medical Research, Chung Shan Medical University Hospital, Taichung,
35
36 15 Taiwan

37
38
39 16
40
41 17 J. H. Chen
42
43 18 Department of Nutrition, Chung Shan Medical University, Taichung, Taiwan

44
45 19
46
47 20 Running title: Carnosic acid induces apoptosis in neuroblastoma cells

48
49 21 **Abbreviations** CA, carnosic acid; JNK, c-Jun NH₂-terminal kinase ; ERK, extracellular
50
51
52 22 signal-regulated kinase ; MAPK, mitogen-activated protein kinase; MTT, 3-(4,
53
54 23 5-dimethylthiazol-2-yl)-2,5-diphenyltetrazolium bromide; NAC, *N*-acetylcysteine; PARP,
55
56
57 24 poly(ADP-ribose) polymerase; PI, propidium iodide; ROS, reactive oxygen species.

58
59 25
60
61

1
2
3
4
5
6
7
8
9
10
11
12
13
14
15
16
17
18
19
20
21
22
23
24
25
26
27
28
29
30
31
32
33
34
35
36
37
38
39
40
41
42
43
44
45
46
47
48
49
50
51
52
53
54
55
56
57
58
59
60
61
62
63
64
65

Abstract Carnosic acid (CA), a rosemary phenolic compound, has been shown to display anti-cancer activity. We examined the apoptotic effect of CA in human neuroblastoma IMR-32 cells and elucidated the role of the reactive oxygen species (ROS) and mitogen-activated protein kinase (MAPK) associated with carcinogenesis. The result indicated that CA decreased the cell viability in a dose-dependent manner. Further investigation in IMR-32 cells revealed that cell apoptosis following CA treatment is the mechanism as confirmed by flow cytometry, hoechst 33258, and caspase-3/-9 and poly(ADP-ribose) polymerase (PARP) activation. Immunoblotting suggested a down-regulation of anti-apoptotic Bcl-2 protein in the CA-treated cells. In flow cytometric analysis, CA caused the generation of reactive oxygen species (ROS); however, pretreatment with the antioxidant *N*-acetylcysteine (NAC) attenuated the CA-induced generation of ROS and apoptosis. This effect was accompanied by increased activation of p38 and by decreased activation of extracellular signal-regulated kinase (ERK) as well as activation of c-Jun NH₂-terminal kinase (JNK). Moreover, NAC attenuated the CA-induced phosphorylation of p38. Silencing of p38 by siRNA gene knockdown reduced the CA-induced activation of caspase-3. In conclusion, ROS-mediated p38 MAPK activation plays a critical role in CA-induced apoptosis in IMR-32 cells.

Keywords Carnosic acid · apoptosis · reactive oxygen species · p38 kinase · human neuroblastoma IMR-32 cells

45 **Introduction**

1
2 46 Neuroblastoma, which is derived from cells of the sympathetic nervous system, is the most
3
4 47 common solid extracranial neoplasm in children [1]. Neuroblastoma is a pediatric tumor that
5
6
7 48 accounts for 15% of childhood cancer deaths and has a poor prognosis in children after 1 year
8
9
10 49 of age [2]. Despite aggressive multimodal therapies, advanced neuroblastoma often acquires
11
12 50 drug resistance and metastasizes [3]. Disruption of the apoptosis machinery plays an
13
14 51 important role in the drug resistance of neuroblastomas. Many chemopreventive agents take
15
16
17 52 effect by inducing apoptosis of neuroblastoma cells [4].
18

19 53 Apoptosis is characterized by morphological changes such as cell membrane blebbing,
20
21 54 cell shrinkage, nuclear condensation, and formation of apoptotic bodies [5]. Activation of
22
23
24 55 caspase is generally considered a hallmark of apoptotic cell death. The active caspase-9
25
26 56 recruits and activates procaspase-3, generating a fragment that activates the mitochondrial
27
28
29 57 pathway. The DNA repair enzyme poly(ADP)-ribose polymerase (PARP) is shown to be
30
31 58 cleaved by caspase-3 and as a result becomes incapable of responding to DNA damage during
32
33
34 59 apoptosis [6, 7].
35

36 60 Recent studies have suggested that reactive oxygen species (ROS) may play an important
37
38
39 61 role during apoptosis induction [8]. Many stimulants such as cigarette smoke, anticancer
40
41 62 drugs, UV irradiation, and chemopreventive agents prompt cells to produce ROS. ROS induce
42
43
44 63 a number of events in mediating apoptosis, including mitogen-activated protein kinases
45
46 64 (MAPKs) signal transduction pathways [9]. Activated MAPKs play key roles in activating
47
48
49 65 transcription factors and downstream kinases, leading to the induction of immediate-early
50
51 66 gene expression and subsequent changes in other cellular processes [10]. The MAPKs are
52
53
54 67 composed of several subfamilies, including the c-Jun NH₂-terminal kinase (JNK),
55
56 68 extracellular signal-regulated kinase (ERK), and p38 kinase. ERK and JNK are activated
57
58
59 69 through receptor-mediated signaling stimuli and are associated with cell proliferation,
60
61
62
63
64
65

1
2
3
4
5
6
7
8
9
10
11
12
13
14
15
16
17
18
19
20
21
22
23
24
25
26
27
28
29
30
31
32
33
34
35
36
37
38
39
40
41
42
43
44
45
46
47
48
49
50
51
52
53
54
55
56
57
58
59
60
61
62
63
64
65

70 differentiation, and survival [11-13]. The p38 pathway is generally activated by stress agents
71 and is implicated as a key regulator of stress-induced apoptosis in different cell types [14].

72 Rosemary (*Rosmarinus officinalis*), a commonly herb or spice, has been reported to
73 possess a number of therapeutic applications in folk medicines. The rosemary phenolic
74 compounds, in particular carnosic acid (CA) , carnosol, and rosmarinic acid, have some
75 biological properties such as antiinflammatory, antioxidative, antiviral, and anticarcinogenic
76 activities [15-18]. CA has been shown to inhibit lipid peroxidation [16] and to protect red
77 cells against oxidative hemolysis [19]. Recently, interest has been growing in the
78 anticarcinogenic properties of CA. Evidence has suggested that the arresting of human
79 colonic adenocarcinoma Caco-2 cells in the G2/M phase by CA was shown to be caused by
80 reduction of cyclin A [20]. In 7,12-dimethylbenz(a)anthracene (DMBA)-induced hamster
81 buccal pouch carcinogenesis model, the chemopreventive potential of CA is probably due to
82 its modulating effect on carcinogen detoxification enzyme [21]. In addition, CA was shown to
83 cause apoptosis and enhance the anticancer activity of vitamin D3 in HL-60 human leukemia
84 cells [22, 23]. Moreover, the combined effect of CA and curcumin on apoptosis in acute
85 myeloid leukemia cells is associated with activation of caspase-8, caspase-9, and caspase-3
86 and the proapoptotic protein Bid [24]. Although CA is considered to be an anti-cancer agent,
87 its particular effects on neuroblastoma IMR-32 cells and the mechanisms involved remain
88 unknown. In this study, we investigated the apoptosis effects of CA in human neuroblastoma
89 IMR-32 cells. Moreover, we determined the involvement of ROS generation and the MAPK
90 pathway in these processes.

92 **Materials and methods**

93 Chemical

94 Carnosic acid, leupeptin, aprotinin, Hoechst 33258 solution, paraformaldehyde,
95 phosphatase inhibitor, HEPES, sodium bicarbonate, EDTA, glycerol, Triton X-100,
96 dimethylsulfoxide (DMSO), sodium pyruvate, 3-(4, 5-dimethylthiazol-2-yl)-2,5-
97 diphenyltetrazolium bromide (MTT), rotenone, ascorbate, and *N*-acetylcysteine (NAC) were
98 obtained from Sigma Chemical Company (St. Louis, MO). MEM medium, L-glutamine,
99 nonessential amino acids, trypsin, sodium bicarbonate, and penicillin-streptomycin solution
100 were obtained from Gibco Laboratory (Grand Island, NY). Fetal bovine serum was purchased
101 from Hyclone (Logan, UT).

103 Cell culture

104 Human neuroblastoma IMR-32 cells were purchased from Bioresources Collection and
105 Research Center (BCRC, Taiwan). IMR-32 cells were grown in MEM medium supplemented
106 with 2 mM L-glutamine, 1.5 g/L sodium bicarbonate, 0.1 mM nonessential amino acids, 1.0
107 mM sodium pyruvate, 1×10^5 unit/L penicillin, 100 mg/L streptomycin, and 10% fetal bovine
108 serum. Cells were incubated at 37°C in a humidified atmosphere of 5% CO₂ and 95% air. For
109 all studies, cells between passages 3 and 10 were used. IMR-32 cells were plated on 35-mm
110 plastic tissue culture dishes (Corning, NY) at a density of 0.7×10^6 cells per dish or on 60-mm
111 plastic tissue culture dishes at a density of 2.5×10^6 cells per dish for Western blot analysis,
112 and the dishes were treated until 70% confluence was reached. Cells were changed to fresh
113 culture medium containing 2.5% fetal bovine serum for 12 h before CA treatment. Different
114 concentrations of CA in 2.5% fetal bovine serum culture medium were then added, and the
115 cells were incubated for the indicated times. Cells treated with 0.1% DMSO alone were
116 regarded as controls. For antioxidant treatments, NAC at a concentration 2 mM and ascorbate

117 at a concentration 1 mM were added 1 h before CA treatment.

118 Cell viability

119 IMR-32 cells were plated on 35-mm plastic tissue culture dishes at a density of 0.7×10^6 cells
120 per dish. Cell viability was determined by the MTT assay. Cells were stimulated with 5, 10,
121 20, 30, and 40 μM of CA for 24 h. MTT solution (5 mg/mL) was added to each dish and the
122 dishes were incubated for 2 h. The formazan product was dissolved by the addition of 1 mL
123 isopropanol to each dish with shaking for 10 min. Absorbance was detected at 570 nm by use
124 of a microplate reader (Bio Rad, Japan).

125

126 Hoechst 33258 staining

127 IMR-32 cells were treated with 5, 10, 20, 30, and 40 μM CA for 24 h. After being washed
128 with phosphate-buffered saline, the cells were fixed with 3.7% paraformaldehyde (pH 7.4) for
129 50 min. Subsequently, Hoechst 33258 nuclear dye was added to a final concentration 5 $\mu\text{g}/\text{mL}$
130 for 1 h at 25°C in the dark. Morphological changes were observed by using a fluorescence
131 microscope.

132

133 Annexin V and propidium iodide (PI) staining

134 IMR-32 cells were exposed to 0.1% DMSO or 30 μM CA for 12, 24, 36, 48, and 60 h. The
135 Annexin V-FITC apoptosis detection kit (Becton Dickinson, San Diego, CA) was used
136 according to the manufacturer's instructions. Following treatment, cells were harvested by
137 trypsinization and washed with warm phosphate-buffered saline, centrifuged at $1,500 \times g$ for 5
138 min at 25°C , and resuspended in 100 μL of 1X binding buffer [10 mM HEPES/NaOH (pH 7.4),
139 140 mM NaCl, and 2.5 mM CaCl_2]. Then Annexin-V FITC and PI were added for 15 min in
140 the dark and finally 400 μL of 1X binding buffer was added. Samples were then immediately
141 analyzed by use of a flow cytometer (Becton Dickinson, Heidelberg, Germany). Acquisition

142 gates of the cells and a minimum of 10,000 events were collected for each sample.
1
2 143 Western blot analysis
3
4 144 IMR-32 cells were washed with cold phosphate-buffered saline and were then harvested in
5
6
7 145 lysis buffer (25 mM Tris-HCl, 150 mM NaCl, 0.5 % Triton X-100, 10% glycerol, 2 mM
8
9
10 146 EDTA, 1 mM PMSF, 1 µg/mL leupeptin, 1 µg/mL aprotinin, and phosphatase inhibitor).
11
12 147 Lysates were centrifuged at 14,000 x g for 20 min at 4°C. Protein concentrations were
13
14 148 measured with a Coomassie plus protein assay reagent kit (Pierce, Rockford, IL). Thirty
15
16 149 micrograms of protein from each sample was applied to 12.5% SDS-PAGE gels and was
17
18
19 150 electrophoretically transferred to polyvinylidene fluoride membranes (Millipore, Bedford,
20
21
22 151 MA). The nonspecific binding sites on the membranes were blocked at 4°C overnight with 50
23
24 152 g/L nonfat dry milk in 25 mM Tris/150 mM NaCl buffer, pH 7.4. The blots were then
25
26
27 153 incubated with primary antibodies against procaspase-3, and -9 or cleaved caspase-3, and -9
28
29 154 or cleaved PARP (all purchased from Cell Signaling Technology, Beverly, MA); β-tubulin
30
31 155 (purchased from Sigma Chemical Company, Louis, MO); JNK1, ERK1/2, phospho-JNK1, or
32
33 156 phospho-ERK1/2 (all from Santa Cruz Biotechnology, Inc., Santa Cruz, CA); p38 (purchased
34
35
36 157 from Cell Signaling Technology, Beverly, MA); or phospho-p38 (purchased from Abcam,
37
38
39 158 Cambridge, UK) overnight at 4°C and were subsequently incubated with horseradish
40
41 159 peroxidase-conjugated goat anti-rabbit IgG or goat anti-mouse IgG. The bands were detected
42
43
44 160 by using an enhanced chemiluminescence kit (all purchased from Perkin Elmer Life Science,
45
46 161 Boston, MA).

47
48
49 162

50
51 163 Measurement of ROS generation

52
53 164 Measurement of intracellular ROS production was made by using the peroxide-sensitive
54
55
56 165 fluorescent probe 2,7-dichlorofluorescein diacetate (DCF-DA) (Molecular Probes Inc., Eugene,
57
58 166 OR) as described previously [25]. In addition, mitochondrial was measured using MitoSOX

167 Red (Invitrogen, Carlsbad, CA). After reaching 90% confluence, cells were changed to fresh
168 culture medium containing 2.5% fetal bovine serum for 12 h before CA treatment. Cells were
169 changed to fresh culture medium containing 2.5% fetal bovine serum and 30 μ M CA for 1, 3,
170 6, and 9 h. For examining the antioxidant effect, cells were pretreated with 2 mM NAC or
171 1mM ascorbate for 1 h and were then co-cultured with 30 μ M CA for 6 h. An amount of 5
172 μ M DCF-DA or 5 μ M MitoSOXTM red were then added to the medium for 45 min before the
173 termination of CA treatment. DCF and MitoSOX Red fluorescence were measured in a flow
174 cytometer (Becton Dickinson, Heidelberg, Germany).

175

176 Transient transfection of small RNA interference

177 IMR-32 cells were seeded at a density of 0.7×10^6 cells/dish in a 35-mm plastic tissue culture
178 dish. When 80% confluence was reached, for p38 small interfering RNA (siRNA) transfection,
179 the cells were transfected with p38-siRNA (100 nM) or nontargeting control siRNA by using
180 the DharmaFECT[®] siRNA transfection reagent according to the manufacturer's instruction
181 (all from Thermo Fisher Scientific, Lafayette, CO) for 12 h. The sense sequences of these p38
182 siRNAs were as follows: 1) 5'-GGACCUCCUUAUAGACGAA-3', 2)
183 5'-GCACACUGAUGACGAAAUG-3', 3) 5'-ACACUCGGCUGACAUAUAUC-3', and 4)
184 5'-GAAUGUGAUUGGUCUGUUG-3'. Twelve hours after transfection, the cells were
185 changed to fresh culture medium containing 2.5% fetal bovine serum and 30 μ M CA for 12 h
186 or 24 h and protein expression was examined by Western blot analysis.

187

188 Statistical analysis

189 Statistical analysis was performed with commercially available software (SAS Institute
190 Inc, Cary, NC). Data were analyzed by means of one-way ANOVA, and the significant
191 difference among treatment means was assessed by use of Tukey's test. Differences between 2

192 groups were assessed using Student's *t* test. Differences were considered significant at *P*

1
2
3
4
5
6
7
8
9
10
11
12
13
14
15
16
17
18
19
20
21
22
23
24
25
26
27
28
29
30
31
32
33
34
35
36
37
38
39
40
41
42
43
44
45
46
47
48
49
50
51
52
53
54
55
56
57
58
59
60
61
62
63
64
65

193 <0.05.

194

195 **Results**

196 CA inhibited cell viability in IMR-32 cells

197 The chemical structure of CA is shown in Fig. 1. First, we investigated the effect of CA
198 treatment on the viability of human neuroblastoma IMR-32 cells. In cells exposed to 5, 10, 20,
199 30, and 40 μM CA for 24 h, cell viability was reduced in a dose-dependent manner ($P < 0.05$)
200 (Fig. 2). CA exhibited potent cytotoxic activity against neuroblastoma IMR-32 cells, with an
201 IC_{50} value of approximately 30 μM .

203 Effect of CA on cell morphology of IMR-32 cells

204 To determine whether the reduced cell viability was due to apoptosis, IMR-32 cells were
205 stained with Hoechst 33258. In the control group, the IMR-32 cells were homogeneously
206 stained (Fig. 3). Nuclear condensation and fragmentation were significantly increased in the
207 cells treated with 30 and 40 μM CA for 24 h. In addition, cells treated with CA were shown to
208 have apoptotic bodies by phase-contrast microscopy.

210 CA induced apoptosis in IMR-32 cells

211 To further confirm the apoptosis, the cells were examined by flow cytometric analysis using
212 double staining of Annexin V-FITC and PI. As shown in Fig. 4, the apoptotic cells were
213 observed in IMR-32 cells treated with CA for 24 h. In the cells treated with CA, the apoptotic
214 population increased gradually throughout the culture period. CA at 60 h increased the
215 apoptotic population by 3.5-fold compared with that of the control cells.

217 CA induced the expression of apoptosis regulatory proteins

218 To clarify the mechanism of CA-induced apoptosis, we examined changes in the caspase
219 family proteins and anti-apoptotic protein Bcl-2 by Western blot analysis. CA significantly

220 reduced procaspase-9 and -3 but markedly increased the cleaved forms of caspase-9, -3, and
221 PARP in a dose-dependent manner (Fig. 5). The ratio of cleaved to procaspase-9 and -3 was
222 increased in the CA-treated group ($P < 0.05$). However, caspase-8 protein was not expressed
223 after cells were treated with CA (data not shown). The level of anti-apoptotic Bcl-2 protein
224 was reduced in cells treated with 30 and 40 μ M CA. These results suggested that the induction
225 of cell death by CA mainly involved activation of the apoptotic mitochondrial pathway.

226

227 Generation of ROS in CA-induced apoptosis

228 We next explored whether ROS generation was involved in the CA-induced apoptosis of
229 IMR-32 cells. The results of the flow cytometry analysis using DCF-DA as a fluorescent ROS
230 indicator showed that intracellular ROS level was gradually increased and reached a
231 maximum at 6 h and then decreased in the presence of CA (Fig. 6A). Compared with the
232 control group, there was a 1.6-fold increase at 6 h. Pretreatment with NAC reduced
233 CA-induced ROS generation by 39%. In addition, we further used the mitochondrial targeted
234 ROS probe-MitoSOX Red to confirm the ROS production. Increases of 2.3 and 2.5 fold in
235 MitoSOX Red fluorescence intensity were noted in cells cultured with CA and rotenone (a
236 mitochondrial inhibitor), respectively, as compared with the control cells. Pretreatment with
237 ascorbate reduced CA-induced mitochondrial ROS generation by 21% (Fig. 6 B).

238 Immunoblots also revealed that CA induced the cleavage of caspase-9, caspase-3, and PARP
239 protein and reduced procaspase-9 and -3 proteins (Fig. 6 C). In contrast, both NAC and
240 ascorbate decreased the CA-induced cleavage of caspase-9, caspase-3, and PARP protein (Fig.
241 6 C). These findings suggested that the generation of ROS may play an important role in the
242 CA-induced apoptosis in IMR-32 cells.

243

244 Role of MAPKs in CA-mediated apoptosis

245 Activation of the MAPK cascades is considered to play a crucial role as a regulator of
1
2 246 apoptotic signaling pathways [9]. Therefore, we attempted to determine whether CA-induced
3
4 247 apoptosis was regulated by JNK1, ERK, and p38 kinase. As shown in Fig. 7 A, the activation
5
6
7 248 of p38 was notably increased after the cells were treated with CA for 12 and 24 h, and
8
9
10 249 returned to basal level after 36 and 48 h. However, the phosphorylation of ERK and JNK1
11
12 250 was decreased in a time-dependent manner (Fig. 7 B). Cells pretreatment with NAC
13
14 251 attenuated the activation of p38 by CA, and had little effect on the phosphorylation of ERK
15
16
17 252 and JNK1. These results suggested that the activation of p38 was mainly involved in the
18
19 253 CA-induced ROS generation.

22 254 To confirm the involvement of p38 activation in the CA-induced apoptosis, we used
23
24 255 knockdown of p38 by siRNA transfection. Immunoblots revealed that CA increased the
25
26
27 256 activation of p38 and caspase-3 (Fig. 8 A). With p38 siRNA, the cellular p38 level was
28
29 257 decreased (vs. si-control), which resulted in alleviation of the phosphorylation of p38 by CA.
30
31 258 The activation of caspase-3 expression by CA was then suppressed (Fig. 8 B).

34 259

36 260

261 **Discussion**

1
2 262 Rosemary extracts have been widely investigated for their antiproliferative and
3
4
5 263 anticarcinogenic properties [26, 27]. Application of rosemary extracts was shown to prevent
6
7 264 DNA damage and tumor formation by 7,12-dimethylbenz[*a*]anthracene in mouse skin and rat
8
9
10 265 mammary gland [26, 28]. The accumulated evidence supports that rosemary extracts inhibit
11
12 266 benzo[*a*]pyrene-induced genotoxicity in human bronchial cells, and the components of
13
14
15 267 rosemary, such as CA, carnosol, and rosmarinic acid, were responsible for this effect [29].
16
17 268 Carnosol displays growth-inhibitory effects in human prostate cancer PC3 cells by G2-phase
18
19 269 cell cycle arrest [17]. Rosmarinic acid induces apoptosis and inhibits the proliferation of
20
21
22 270 human HCT115 colorectal cells via MAPK/ERK pathway [30]. In human colon
23
24 271 adenocarcinoma COLO 205 cells, the rosmanol extracted from rosemary is capable of
25
26
27 272 inducing apoptosis through both a mitochondria-mediated pathway and a receptor-mediated
28
29 273 pathway [31]. Recent studies have suggested that CA inhibits the proliferation of Caco-2 cells
30
31
32 274 by causing cell cycle arrest at the G2/M phase and induces apoptosis in human promyelocytic
33
34 275 leukemia HL-60 cells [20, 23]. Moreover, the combinatorial effect of CA and curcumin on
35
36 276 apoptosis in acute myeloid leukemia cells was associated with activation of caspase-9 and
37
38
39 277 caspase-3 and the pro-apoptotic protein Bid [24]. The results of the present study suggest that
40
41 278 CA induced the apoptosis of IMR32 neuroblastoma cells via the mitochondrial pathway. We
42
43
44 279 suggest that the generation of ROS by CA leads to activation of the p38 pathway, which
45
46 280 results in apoptosis.

47
48 281 Caspases are a family of cysteine proteases that play a central role during the executional
49
50
51 282 phase of apoptosis. Several chemotherapeutic drugs induce cell death through the
52
53 283 caspase-mediated apoptosis pathways. Activation of caspase-8 is via the extrinsic apoptosis
54
55
56 284 pathway, which is induced by triggering of the death receptors pathway. Our results indicated
57
58 285 that caspase-8 protein was not expressed after cells were treated with CA for 24 h (data not
59
60
61
62
63
64
65

286 shown). This finding is supported by the findings of others that some neuroblastoma cell lines
1
2 287 such as IMR-32 do not express caspase-8 protein [32]. Moreover, loss of caspase-8
3
4 288 expression has been reported in patients with highly malignant neuroblastoma [33]. In the
5
6
7 289 intrinsic apoptosis pathway, upon apoptotic stimulation, initiator caspases such as caspase-9
8
9
10 290 are cleaved and activated. The activated upstream caspases further process the downstream
11
12 291 executioner caspases, such as caspase-3 and -7, by cleaving them into large and small
13
14 292 subunits, thereby initiating a caspase cascade leading to apoptosis [7]. The Bcl-2 family
15
16 293 proteins, the pro-apoptotic Bax and the anti-apoptotic Bcl-2, regulate cell death by controlling
17
18 294 mitochondrial membrane permeability during apoptosis [34]. A decrease in the levels of Bcl-2
19
20
21 295 leads to the loss of mitochondrial transmembrane potential, a key event in the induction of
22
23
24 296 apoptosis, and opens mitochondrial permeability transition pores [35]. Isobavachalcone, a
25
26 297 chalcone constituent of *Angelica keiskei*, induces apoptotic cell death with caspase-3 and -9
27
28
29 298 activation and Bax upregulation in neuroblastoma IMR-32 and NB-39 cells [32]. Zn
30
31 299 deficiency triggers IMR-32 apoptotic death associated with the intrinsic pathway, which can
32
33
34 300 be a consequence of ERK inhibition and caspase-3 activation [36]. However, xanthoangelol,
35
36 301 another chalcone constituent of *Angelica keiskei*, induces apoptotic cell death by activation of
37
38
39 302 caspase-3 in neuroblastoma IMR-32 cells through a mechanism that does not involve
40
41 303 Bax/Bcl-2 signal transduction [37]. In the present study, both CA and rotenone induced
42
43
44 304 apoptotic cell death with Bcl-2 downregulation and caspase-9 and caspase-3 activation,
45
46 305 resulting in cleavage of PARP in IMR32 neuroblastoma cells (Fig. 5). Taken together, these
47
48
49 306 results indicate that the CA-induced cell death involved activation of the apoptotic
50
51 307 mitochondrial pathway.

52
53 308 Recent studies have indicated that cancer chemopreventive agents induce apoptosis in
54
55
56 309 part by the generation of ROS and the disruption of redox homeostasis [38]. The generation of
57
58
59 310 ROS induces mitochondrial cytochrome *c* release, in which sequential activation of caspase-9

311 and -3 occurs [39]. The induction of apoptosis by garlic diallyl disulfide is associated with the
312 production of ROS and activation of caspase-3 in Ca Ski cells [40]. In addition, surfactin
313 induces apoptosis in human breast cancer MCF-7 cells through a ROS-mediated
314 mitochondrial/caspase pathway [41]. In the present study, we monitored the change in cellular
315 redox status by the DCF-DA and MitoSOX Red cytofluorimetric assay. With CA treatment,
316 ROS production gradually increased and reached a maximum at 6 h and then decreased (Fig.
317 6 A) Moreover, this effect was reduced by pretreatment with NAC and ascorbate. This
318 suggests that the activation of the apoptosis caspase cascade can be explained, at least in part,
319 by a change in redox states caused by CA (Fig. 6 C).

320 MAPKs control many cellular events, including differentiation, proliferation, and
321 apoptosis [12, 14, 42]. JNK regulates serotonin-mediated proliferation and migration in
322 pulmonary artery smooth muscle cells [12]. Treatment of IMR-32 cells with CdSe-core
323 induces mitochondrial-dependent apoptotic processes by inhibiting ERK survival signaling
324 [13]. Xavier and co-workers presented that rosmarinic acid induces apoptosis and inhibits the
325 proliferation of human HCT115 colorectal cells via inhibition of the ERK pathway [30]. In
326 particular, p38 is known to play a critical role in the transmission of apoptotic signals [43].
327 Indole ethyl isothiocyanate is thought to inhibit the cell proliferation and cell viability of
328 neuroblastoma SMS-KCNR through activation of p38 signaling [14]. The p38 MAPK
329 pathway is also critical for 5,5'-dibromodiindolylmethane-induced apoptosis to prevent oral
330 squamous carcinoma cells [42]. These findings agree with our results that IMR-32 cells
331 treated with CA activated p38 protein and down-regulated ERK1/2 and JNK protein (Fig. 7A).
332 Furthermore, the CA-induced activation of p38 through a ROS-dependent mechanism was
333 evidenced by inhibition of p38 phosphorylation by NAC (Fig. 7 B). Pretreatment with p38
334 siRNA attenuated the activation of p38 and caspase-3 by CA (Fig. 8 A and 8 B). These data
335 suggest that the p38 pathway played an important role in the generation of ROS by CA, which

336 induced apoptosis of IMR-32 cells. This explanation is similar by the finding that the
1
2 337 activation of the p38 signaling pathway by arachidonic acid and the resulting induction of
3
4
5 338 human leukemia U937 cell apoptosis are prevented by NAC [38].
6

7 339 In conclusion, the results of the present study indicate that CA induces apoptotic cell
8
9
10 340 death through the mitochondrial pathway in human neuroblastoma IMR-32 cells. Moreover,
11
12 341 ROS-mediated phosphorylation of p38 could play a critical role in CA-induced apoptosis.
13

14 342
15
16
17
18
19
20
21
22
23
24
25
26
27
28
29
30
31
32
33
34
35
36
37
38
39
40
41
42
43
44
45
46
47
48
49
50
51
52
53
54
55
56
57
58
59
60
61
62
63
64
65

343 **Acknowledgment**

1
2
3
4
5
6
7
8
9
10
11
12
13
14
15
16
17
18
19
20
21
22
23
24
25
26
27
28
29
30
31
32
33
34
35
36
37
38
39
40
41
42
43
44
45
46
47
48
49
50
51
52
53
54
55
56
57
58
59
60
61
62
63
64
65

344 This work was supported by China Medical University (CMU) (grant no. CMU97-246).

345

346 **References**

- 1 347
- 2 348 1. Nakagawara A, Ohira M (2004) Comprehensive genomics linking between neural
- 3 349 development and cancer: neuroblastoma as a model. *Cancer Lett* 204:213-224
- 4 350 2. Torkin R, Lavoie JF, Kaplan DR *et al* (2005) Induction of caspase-dependent,
- 5 351 p53-mediated apoptosis by apigenin in human neuroblastoma. *Mol Cancer Ther* 4:1-11
- 6 352 3. Brard L, Singh RK, Kim KK *et al* (2009) Induction of cytotoxicity, apoptosis and cell
- 7 353 cycle arrest by 1-t-butyl carbamoyl, 7-methyl-indole-3-ethyl isothiocyanate (NB7M) in
- 8 354 nervous system cancer cells. *Drug Des Devel Ther* 2:61-69
- 9 355 4. Fulda S (2009) Apoptosis pathways and neuroblastoma therapy. *Curr Pharm Des*
- 10 356 15:430-435
- 11 357 5. Blum D, Torch S, Lambeng N *et al* (2001) Molecular pathways involved in the
- 12 358 neurotoxicity of 6-OHDA, dopamine and MPTP: contribution to the apoptotic theory in
- 13 359 Parkinson's disease. *Prog Neurobiol* 65:135-172
- 14 360 6. Carter R, Sykes V, Lanning D (2009) Scarless fetal mouse wound healing may initiate
- 15 361 apoptosis through caspase 7 and cleavage of PARP. *J Surg Res* 156:74-79
- 16 362 7. Strahlendorf J, Box C, Attridge J *et al* (2003) AMPA-induced dark cell degeneration of
- 17 363 cerebellar Purkinje neurons involves activation of caspases and apparent mitochondrial
- 18 364 dysfunction. *Brain Res* 994:146-159
- 19 365 8. Sahu RP, Zhang R, Batra S *et al* (2010) Benzyl isothiocyanate-mediated generation of
- 20 366 reactive oxygen species causes cell cycle arrest and induces apoptosis via activation of
- 21 367 MAPK in human pancreatic cancer cells. *Carcinogenesis* 30:1744-1753
- 22 368 9. Deng YT, Huang HC, Lin JK (2009) Rotenone induces apoptosis in MCF-7 human breast
- 23 369 cancer cell-mediated ROS through JNK and p38 signaling. *Mol Carcinog* 49:141-151
- 24 370 10. Kyriakis JM, Avruch J (2001) Mammalian mitogen-activated protein kinase signal
- 25 371 transduction pathways activated by stress and inflammation. *Physiol Rev* 81:807-869
- 26 372 11. Vauzour D, Vafeiadou K, Rice-Evans C *et al* (2007) Activation of pro-survival Akt and
- 27 373 ERK1/2 signalling pathways underlie the anti-apoptotic effects of flavanones in cortical
- 28 374 neurons. *J Neurochem* 103:1355-1367
- 29 375 12. Wei L, Liu Y, Kaneto H *et al* (2010) C-Jun N-terminal Kinase (JNK) Regulates
- 30 376 Serotonin-mediated Proliferation and Migration of Pulmonary Artery Smooth Muscle
- 31 377 Cells. *Am J Physiol Lung Cell Mol Physiol* in press
- 32 378 13. Chan WH, Shiao NH, Lu PZ (2006) CdSe quantum dots induce apoptosis in human
- 33 379 neuroblastoma cells via mitochondrial-dependent pathways and inhibition of survival
- 34 380 signals. *Toxicol Lett* 167:191-200
- 35 381 14. Singh RK, Lange TS, Kim K *et al* (2007) Effect of indole ethyl isothiocyanates on
- 36 382 proliferation, apoptosis, and MAPK signaling in neuroblastoma cell lines. *Bioorg Med*
- 37 383 *Chem Lett* 17:5846-5852
- 38 384 15. Posadas SJ, Caz V, Largo C *et al* (2009) Protective effect of supercritical fluid rosemary
- 39 385 extract, *Rosmarinus officinalis*, on antioxidants of major organs of aged rats. *Exp*
- 40 386 *Gerontol* 44:383-389
- 41 387 16. Wijeratne SS, Cuppett SL (2007) Potential of rosemary (*Rosmarinus officinalis* L.)
- 42 388 diterpenes in preventing lipid hydroperoxide-mediated oxidative stress in Caco-2 cells. *J*
- 43 389 *Agric Food Chem* 55:1193-1199
- 44 390 17. Johnson JJ, Syed DN, Heren CR *et al* (2008) Carnosol, a dietary diterpene, displays
- 45 391 growth inhibitory effects in human prostate cancer PC3 cells leading to G2-phase cell
- 46 392 cycle arrest and targets the 5'-AMP-activated protein kinase (AMPK) pathway. *Pharm*
- 47 393 *Res* 25:2125-2134
- 48 394 18. Aruoma OI, Spencer JP, Rossi R *et al* (1996) An evaluation of the antioxidant and
- 49 395 antiviral action of extracts of rosemary and Provençal herbs. *Food Chem Toxicol*
- 50
- 51
- 52
- 53
- 54
- 55
- 56
- 57
- 58
- 59
- 60
- 61
- 62
- 63
- 64
- 65

- 396 34:449-456
- 1 397 19. Haraguchi H, Saito T, Okamura N *et al* (1995) Inhibition of lipid peroxidation and
2 398 superoxide generation by diterpenoids from *Rosmarinus officinalis*. *Planta Med*
3 399 61:333-336
- 4 400 20. Visanji JM, Thompson DG, Padfield PJ (2006) Induction of G2/M phase cell cycle arrest
5 401 by carnosol and carnosic acid is associated with alteration of cyclin A and cyclin B1
6 402 levels. *Cancer Lett* 237:130-136
- 7 403 21. Manoharan S, Vasanthaselman M, Silvan S *et al* (2010) Carnosic acid: a potent
8 404 chemopreventive agent against oral carcinogenesis. *Chem Biol Interact* 188:616-622
- 9 405 22. Sharabani H, Izumchenko E, Wang Q *et al* (2006) Cooperative antitumor effects of
10 406 vitamin D3 derivatives and rosemary preparations in a mouse model of myeloid leukemia.
11 407 *Int J Cancer* 118:3012-3021
- 12 408 23. Wang R, Li H, Guo G *et al* (2008) Augmentation by carnosic acid of apoptosis in human
13 409 leukaemia cells induced by arsenic trioxide via upregulation of the tumour suppressor
14 410 PTEN. *J Int Med Res* 36:682-690
- 15 411 24. Pesakhov S, Khanin M, Studzinski GP *et al* (2010) Distinct combinatorial effects of the
16 412 plant polyphenols curcumin, carnosic acid, and silibinin on proliferation and apoptosis in
17 413 acute myeloid leukemia cells. *Nutr Cancer* 62:811-824
- 18 414 25. Tsai CW, Chen HW, Yang JJ *et al* (2007) Diallyl disulfide and diallyl trisulfide
19 415 up-regulate the expression of the pi class of glutathione S-transferase via an
20 416 AP-1-dependent pathway. *J Agric Food Chem* 55:1019-1026
- 21 417 26. Sancheti G, Goyal PK (2006) Effect of *Rosmarinus officinalis* in modulating
22 418 7,12-dimethylbenz(a)anthracene induced skin tumorigenesis in mice. *Phytother Res*
23 419 20:981-986
- 24 420 27. Cheung S, Tai J (2007) Anti-proliferative and antioxidant properties of rosemary
25 421 *Rosmarinus officinalis*. *Oncol Rep* 17:1525-1531
- 26 422 28. Singletary K, MacDonald C, Wallig M (1996) Inhibition by rosemary and carnosol of
27 423 7,12-dimethylbenz[a]anthracene (DMBA)-induced rat mammary tumorigenesis and in
28 424 vivo DMBA-DNA adduct formation. *Cancer lett* 104:43-48
- 29 425 29. Offord EA, Mace K, Ruffieux C *et al* (1995) Rosemary components inhibit
30 426 benzo[a]pyrene-induced genotoxicity in human bronchial cells. *Carcinogenesis*
31 427 16:2057-2062
- 32 428 30. Xavier CP, Lima CF, Fernandes-Ferreira M *et al* (2009) *Salvia fruticosa*, *Salvia*
33 429 *officinalis*, and rosmarinic acid induce apoptosis and inhibit proliferation of human
34 430 colorectal cell lines: the role in MAPK/ERK pathway. *Nutr Cancer* 61:564-571
- 35 431 31. Cheng AC, Lee MF, Tsai ML *et al* (2010) Rosmanol potently induces apoptosis through
36 432 both the mitochondrial apoptotic pathway and death receptor pathway in human colon
37 433 adenocarcinoma COLO 205 cells. *Food Chem Toxicol* in press
- 38 434 32. Nishimura R, Tabata K, Arakawa M *et al* (2007) Isobavachalcone, a chalcone constituent
39 435 of *Angelica keiskei*, induces apoptosis in neuroblastoma. *Biol Pharm Bull* 30:1878-1883
- 40 436 33. Stupack DG, Teitz T, Potter MD *et al* (2006) Potentiation of neuroblastoma metastasis by
41 437 loss of caspase-8. *Nature* 439:95-99
- 42 438 34. Danial NN, Korsmeyer SJ (2004) Cell death: critical control points. *Cell* 116:205-219
- 43 439 35. Szigeti A, Hocsak E, Rapolti E *et al* (2010) Facilitation of mitochondrial outer and inner
44 440 membrane permeabilization and cell death in oxidative stress by a novel Bcl-2 homology
45 441 3 domain protein. *J Biol Chem* 285:2140-2151
- 46 442 36. Adamo AM, Zago MP, Mackenzie GG *et al* (2010) The role of zinc in the modulation of
47 443 neuronal proliferation and apoptosis. *Neurotox Res* 17:1-14
- 48 444 37. Tabata K, Motani K, Takayanagi N *et al* (2005) Xanthoangelol, a major chalcone
49 445 constituent of *Angelica keiskei*, induces apoptosis in neuroblastoma and leukemia cells.
- 50
51
52
53
54
55
56
57
58
59
60
61
62
63
64
65

- 446 Biol Pharm Bull 28:1404-1407
- 1 447 38. Chen KC, Chang LS (2009) Arachidonic acid-induced apoptosis of human neuroblastoma
2 448 SK-N-SH cells is mediated through mitochondrial alteration elicited by ROS and
3 449 Ca(2+)-evoked activation of p38alpha MAPK and JNK1. Toxicology 262:199-206
- 4 450 39. Takahashi A, Masuda A, Sun M *et al* (2004) Oxidative stress-induced apoptosis is
5 451 associated with alterations in mitochondrial caspase activity and Bcl-2-dependent
6 452 alterations in mitochondrial pH (pHm). Brain Res Bull 62:497-504
- 7 453 40. Lin YT, Yang JS, Lin SY *et al* (2008) Diallyl disulfide (DADS) induces apoptosis in
8 454 human cervical cancer Ca Ski cells via reactive oxygen species and Ca2+-dependent
9 455 mitochondria-dependent pathway. Anticancer Res 28:2791-2799
- 10 456 41. Cao XH, Wang AH, Wang CL *et al* (2010) Surfactin induces apoptosis in human breast
11 457 cancer MCF-7 cells through a ROS/JNK-mediated mitochondrial/caspase pathway. Chem
12 458 Biol Interact 183:357-362
- 13 459 42. Choi KH, Kim HK, Kim JH *et al* (2010) The p38 MAPK pathway is critical for
14 460 5,5'-dibromodiindolylmethane-induced apoptosis to prevent oral squamous carcinoma
15 461 cells. Eur J Cancer Prev 19:153-159
- 16 462 43. Tikhomirov O, Carpenter G (2004) Ligand-induced, p38-dependent apoptosis in cells
17 463 expressing high levels of epidermal growth factor receptor and ErbB-2. J Biol Chem
18 464 279:12988-12996
- 19 465
- 20
- 21
- 22
- 23
- 24
- 25
- 26
- 27
- 28
- 29
- 30
- 31
- 32
- 33
- 34
- 35
- 36
- 37
- 38
- 39
- 40
- 41
- 42
- 43
- 44
- 45
- 46
- 47
- 48
- 49
- 50
- 51
- 52
- 53
- 54
- 55
- 56
- 57
- 58
- 59
- 60
- 61
- 62
- 63
- 64
- 65

466

1 467 **Fig. 1** Chemical structure of carnosic acid (CA).

2

3 468 **Fig. 2** Carnosic acid (CA) inhibited cell growth in human neuroblastoma IMR-32 cells.

4

5 469 IMR-32 cells were treated with 0.1% dimethylsulfoxide (DMSO) alone (control, -) or with

6

7 470 10, 20, 30, or 40 μ M of CA for 24 h. Cell viability was assessed by using the

8

9 471 3-(4,5-dimethylthiazol-2-yl)-2,5-diphenyltetrazolium bromide (MTT) assay. The level in the

10

11 472 control cells was set at 100%. Values are shown as the means \pm SD of four independent

12

13 473 experiments. Means without a common letter differ, $P < 0.05$.

14

15 474

16

17 475 **Fig. 3** Carnosic acid (CA) induces nuclear morphology changes in human neuroblastoma

18

19 476 IMR-32 cells. Nuclei were visualized with Hoechst 33258 staining. Cells were treated with

20

21 477 0.1% dimethylsulfoxide (DMSO) alone (control, -) or with 5, 10, 20, 30, or 40 μ M of CA

22

23 478 for 24 h. Upper panels show the phase contrast image and lower panels show the fluorescent

24

25 479 image. Phase contrast and fluorescent images were obtained from the same view

26

27 480 (magnification, 200 x). Arrows indicate apoptotic cells. One representative image out of four

28

29 481 independent experiments is shown.

30

31 482

32

33 483 **Fig. 4** Carnosic acid (CA) induces apoptosis in human neuroblastoma IMR-32 cells. Cells

34

35 484 were exposed to the medium with 0.1% dimethylsulfoxide (DMSO) alone (control, -) or

36

37 485 with 30 μ M CA for 12, 24, 36, 48, and 60 h. Cell distribution was analyzed by using Annexin

38

39 486 V-FITC binding and propidium iodide (PI) uptake as described in the Materials and Methods.

40

41 487 FITC and PI fluorescence were measured by flow cytometry. In these dot graphs, Q1-1

42

43 488 indicates necrotic cells (Annexin V⁻/PI⁺), Q2-1 indicates late apoptotic cells (Annexin V⁺/PI⁺),

44

45 489 Q3-1 indicates viable cells (Annexin V⁻/PI⁻), and Q4-1 indicates early apoptotic cells

46

47

48

49

50

51

52

53

54

55

490 (Annexin V⁺/PI). Bars are the percentage of early and late apoptotic cells. Values are
491 expressed as the means±SD of three representative experiments. Groups not sharing a
492 common letter differ significantly, $P < 0.05$.

Fig. 5 Carnosic acid (CA) dose-dependently increased apoptotic regulatory proteins in human
neuroblastoma IMR-32 cells. Cells were treated with 0.1% dimethylsulfoxide (DMSO) alone
(control, -) or with 10, 20, 30, or 40 μ M CA for 24 h to determine the protein levels. The
cleaved caspase/procaspase ratio relative to the control group (mean±SD) is shown.
Normalization of Western blots was ensured by β -tubulin. The level in control cells was
regarded as 1. Means without a common letter differ, $P < 0.05$. One representative
immunoblot out of four independent experiments is shown.

Fig. 6 Carnosic acid (CA)-induced apoptosis is associated with the generation of intracellular
reactive oxygen species (ROS) in human neuroblastoma IMR-32 cells. Cells were cultured
with 0.1% dimethylsulfoxide (DMSO) alone (control, -) or with 30 μ M of CA for 1, 3, 6,
and 9 h, or with 50 μ M of rotenone for 6 h. For examining the antioxidant effect, cells were
pretreated with 2 mM NAC or 1 mM ascorbate for 1 h and then co-cultured with CA for 6 h.
(a) DCF fluorescence and (b) MitoSOX Red fluorescence were measured by flow cytometry.
The level in the control cells was set at 1. Values are shown as the means±SD of four
independent experiments. Means without a common letter differ significantly, $P < 0.05$.
*Different from CA or rotenone alone in control group, $P < 0.05$. #Different from CA
co-cultured with ascorbate in CA alone group, $P < 0.05$. (c) The expression of indicated
proteins was analyzed by Western blotting. One representative immunoblot out of four
independent experiments is shown.

514

1
2 **Fig. 7** Effect of carnosic acid (CA) on the activation of ERK1/2, JNK1, and p38 in human
3
4
5 516 neuroblastoma IMR-32 cells. Cells were cultured with 0.1% dimethylsulfoxide (DMSO)
6
7 517 alone (control, -) or with 30 μ M of CA for 12, 24, 36, and 48 h. (a) Activation of ERK1/2,
8
9
10
11 518 JNK1, and p38 was assessed by immunoblot analysis of the phosphorylated forms (P-) of the
12
13 519 mitogen-activated protein kinases in whole cell lysates. β -Tubulin was used as the loading
14
15
16 520 control. (b) The expression of indicated proteins was analyzed after incubation with CA for 12
17
18 521 h in the presence or absence of NAC, which was added to cells 1 h before CA treatment. One
19
20
21 522 representative immunoblot out of three independent experiments is shown.

22
23 523

24
25 **Fig. 8** Carnosic acid (CA)-induced activation of caspase-3 was inhibited by p38-siRNA in
26
27 525 human neuroblastoma IMR-32 cells. Cells were transfected with p38-siRNA (si-p38) or
28
29
30 526 nontargeting control siRNA (si-control) for 12 h. The transfected cells were then treated with
31
32 527 30 μ M of CA for 12 and 24 h. The activation of p38 and capase-3 were measured by Western
33
34
35 528 blotting. β -tubulin was used as the loading control. One representative immunoblot out of
36
37 529 three independent experiments is shown.

Fig. 1

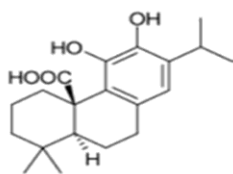


Fig. 2

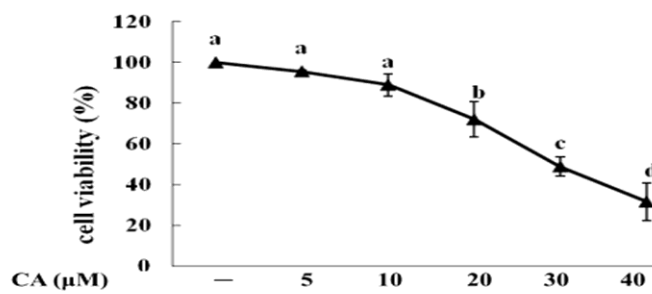


Fig. 3

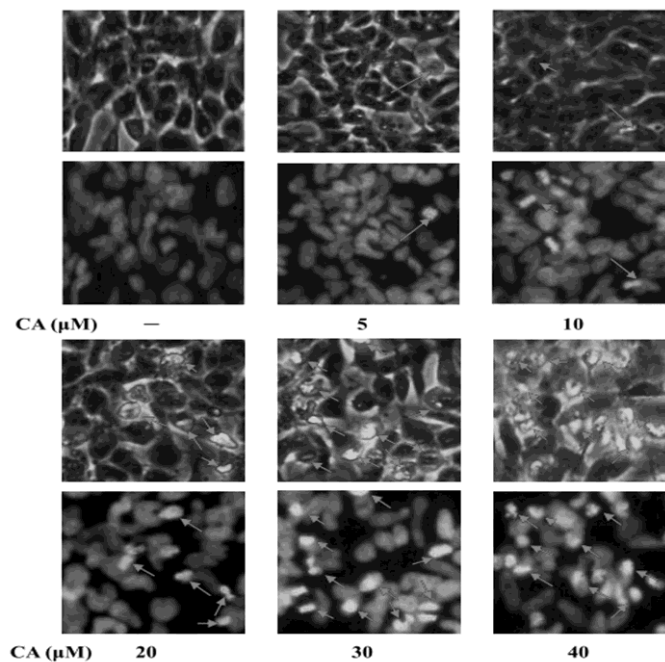


Fig. 4

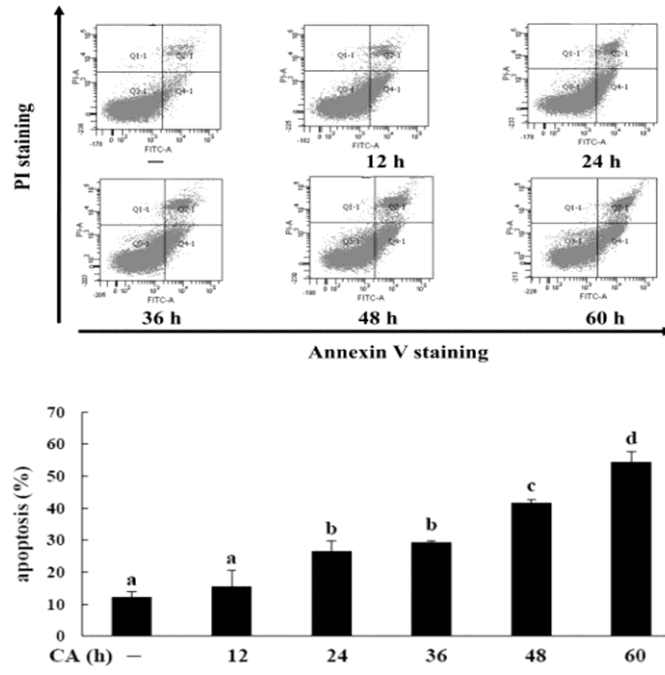


Fig. 5

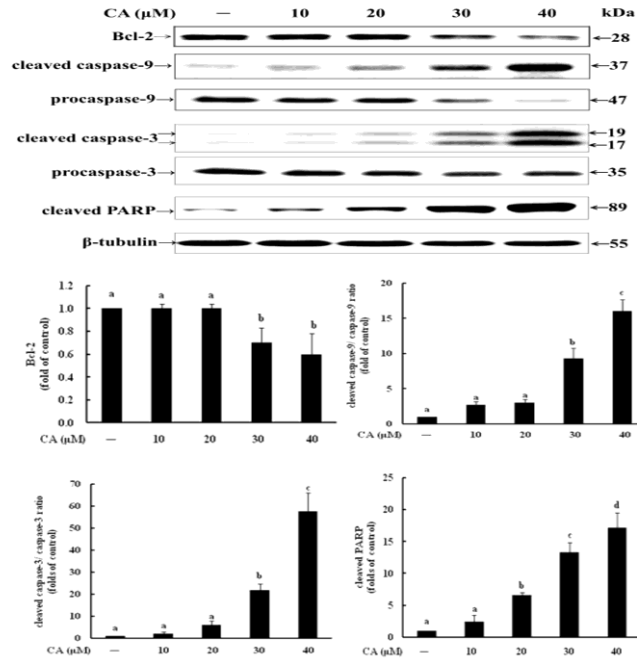


Fig. 6

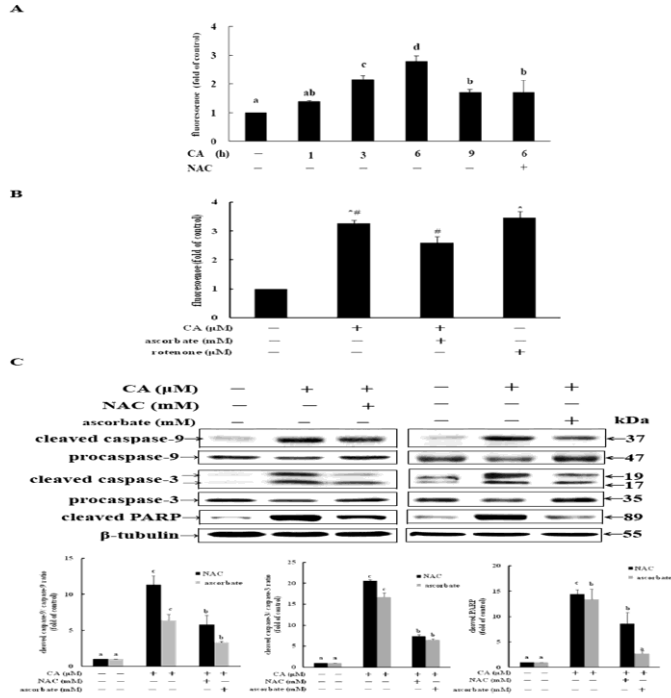


Fig. 7

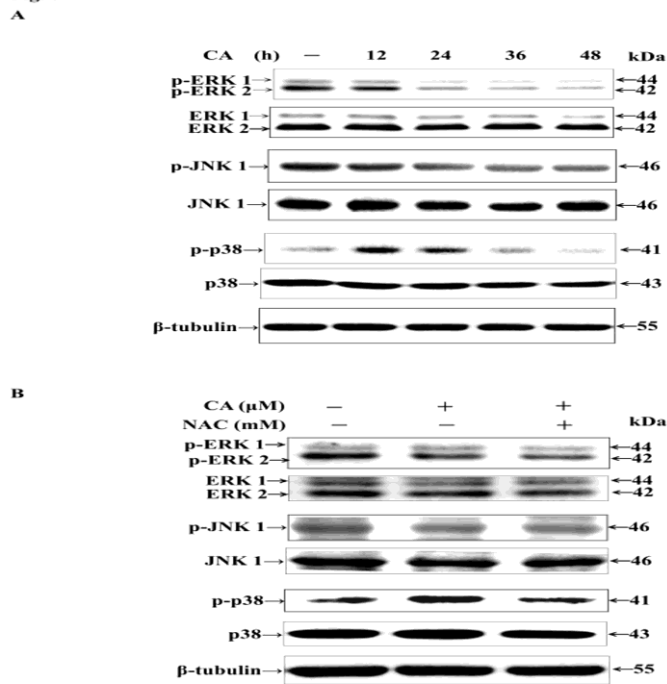
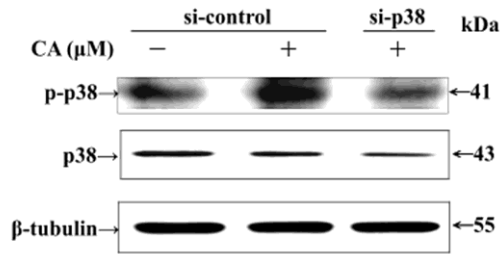


Fig. 8

A



B

